Helium-atom-scattering study of multiphonon processes on LiF(001)⟨100⟩ with temperature variation for specular and off-specular angles

G. G. Bishop, E. S. Gillman, Jeff Baker, J. J. Hernández, S. A. Safron, and J. G. Skofronick

Department of Physics, Department of Chemistry, and Center for Materials Science Research and Development (MARTECH), Florida State University, Tallahassee, Florida 32306

Srilal M. Weera and J. R. Manson

Department of Physics and Astronomy, Clemson University, Clemson, South Carolina 29634

(Received 10 April 1995)

High-resolution inelastic He-atom-scattering experiments, employing a time-of-flight energy resolution technique, have been carried out on LiF(001)⟨100⟩ for a wide range of temperatures and for several different incident beam angles. A quantum-mechanical multiphonon theory is used to explain the observed inelastic background. Numerical calculations based on the theory produce good agreement with experiment.

I. INTRODUCTION

The first gas-surface diffraction experiments using atomic and molecular beams were carried out in the early 1930s to verify the wave nature of atoms.[1-3] Single-crystal LiF(100) was used for most of these early studies, since its cleaved surface remains clean and ordered, and the scattering from it produces a strong diffraction pattern due to the highly corrugated surface. Thermal-energy helium gas was used as the beam probe not only because it is inert and nondestructive to the surface but primarily because of its relatively small mass which insures a de Broglie wavelength similar to the unit-cell size of the LiF crystal. The interesting observations made in those pioneering studies were soon followed by various experimental and theoretical attempts to learn more about atom-surface scattering.[4-6]

With improved vacuum conditions, the field blossomed during the 1960s and 1970s.[7-10] More recently, the development of high-intensity nearly monoenergetic helium-atom beams has spurred further interest in gas-surface interactions. Subsequent developments over the last fifteen years have contributed to making He-scattering studies an exceptionally versatile tool for surface studies. Today's high-resolution atomic He beams can routinely achieve beam velocity spreads of less than 1% and, with care, resolve features below 0.1 meV.[11-14] These experimental and theoretical attempts are discussed in a number of review articles.[15-24]

In the scattering of He from a clean crystal surface, such as LiF, the scattered beam is composed of (1) coherent elastic scattering (specular and Bragg peaks), (2) coherent single-phonon inelastic scattering (single-phonon interactions from surface- or bulk-projected phonons), (3) incoherent elastic or diffuse elastic scattering (from defects), and (4) diffuse inelastic scattering. This paper is mainly concerned with the last of these. The diffuse inelastic scattering appears as a broad background in the experimental energy exchange spectra, especially at higher incident beam energies and elevated crystal surface temperatures, and consists of two parts, incoherent inelastic scattering from defects[25] and coherent multiphonon interactions. For clean, well-ordered surfaces the multiphonon contribution usually dominates. Although this component of the scattering background has a broad shape, it is not featureless. For example, it has been recognized that multiphonon processes are responsible for certain peaks observed in the inelastic spectrum of He scattering.[26] Moreover, a good knowledge of the form and shape of the diffuse inelastic signal is essential for background subtraction in order to obtain the true intensities of the elastic and single-phonon peaks.

In principle, the surface phonon spectral density which depends on the surface bonding forces can be obtained from measurements of the intensities from single-phonon scattering collisions. However, this information can be extracted only when the influence of the He-surface interaction potential is understood since the scattering intensity depends on both the spectral density and the interaction potential. Since the multiphonon contribution is a collective average of the effects of exchanging several phonons, it is not strongly dependent on the details of the phonon spectral density. As a result one can approximate the multiphonon scattering with simple phonon models, such as the Debye model, in order to extract the form factor for the interaction potential that couples the projectile to the surface. Then one can use the form factor from the multiphonon scattering to obtain the phonon spectral density from the single-phonon scattering intensities.

In this study, the variation of the scattered intensity with crystal temperature as well as with the angle of incidence of the He beam was measured. The temperatures ranged from approximately 290 to 720 K. Since the bulk Debye temperature for LiF is 734 K,[27] the inelastic intensity consists mostly of single phonons at the lower end of the temperature range investigated. At higher temperatures, however, the multiphonon contribution is quite significant and we have been able to obtain reasonable agreement between the observed multiphonon scattering and the theoretical predictions.

    <u>52</u>   13 229

The next section contains a description of the apparatus and kinematical conditions that describe the scattering processes in these studies. This is followed by a review of the theory used to model the experimental results. Section IV contains a discussion of the results of the modeling, which is followed in Sec. V by the conclusions.

II. EXPERIMENT

The experimental work for this study was conducted on a helium-atom-scattering (HAS) apparatus that has been described previously.[28] Briefly, this instrument is designed with a 90° source-target-detector scattering geometry. The source is a high-intensity, nearly monoenergetic ($\Delta E/E \approx 2\%$) He beam. The detector is a quadrupole mass spectrometer. The inelastic scattering intensity is measured by chopping the beam into 7 μs pulses and using the time-of-flight (TOF) method to determine the energies and momenta of the scattered atoms.[23–29]

LiF was used in this work because it is a crystalline material which can be cleaved in air to produce a nearly defect-free surface that has been well characterized by previous diffractive and inelastic atom-scattering studies.[15,24] After cleaving, the LiF target ($7 \times 7 \times 2$ mm^3) was immediately inserted into the scattering chamber which was then evacuated and baked at about 370 K for 24 h, by which time the pressure had dropped to below 5×10^{-10} torr. The target temperature was then raised to 770 K for approximately 30 min to clean the surface. Following this treatment, the helium-atom scattering yielded angular distributions with sharp diffraction peaks and inelastic TOF peaks that agreed with previous measurements.[29–31]

The crystal temperatures in these studies were varied from about 290 to 720 K. Although the temperature was allowed to stabilize for each measurement, variations still occurred which ranged from a few tenths of a kelvin at 290 K up to approximately ±5 K at 700 K during a typical 2 h TOF measurement. Since the temperature of the crystal was measured at the position of the stage onto which the crystal was mounted, it is likely that the recorded temperature is slightly different from that of the surface, especially at the higher temperatures. We have made no attempt to correct for this.

For an incoming helium atom of mass m and wave vector $\mathbf{k}_i$ the incident energy E_i is

$$E_i = \frac{\hbar^2 \mathbf{k}_i^2}{2m}. \qquad (1)$$

Similarly, the scattered He atom with a wave vector k_f has energy E_f given by

$$E_f = \frac{\hbar^2 \mathbf{k}_f^2}{2m}. \qquad (2)$$

The helium atom may scatter from the surface with the creation or annihilation of one or more phonons of frequency $\omega(\mathbf{Q})$, where $\mathbf{Q}$ is the surface projection of the phonon wave vector q. The conservation of momentum in the crystal plane and energy conservation then yield

$$K = K_f - K_i = G_{mn} + \sum_l Q_l, \qquad (3)$$

and

$$\Delta E = \frac{\hbar^2 \mathbf{k}_f^2}{2m} - \frac{\hbar^2 \mathbf{k}_i^2}{2m} = \hbar \sum_l \omega_l(Q), \qquad (4)$$

where capital letters denote vector components in the surface plane, ΔE is the energy transfer to the particle, $\mathbf{K}$ is the parallel momentum transferred to the crystal by the particle, l is an index of the phonons exchanged during a single scattering event, and the convention is used that for annihilation events $\omega_l > 0$ and for creation events $\omega_l < 0$. The reciprocal lattice vector $\mathbf{G}_{mn}$ is given, for the (001) surface of a face-centered cubic lattice, by

$$\mathbf{G}_{mn} = \frac{2\pi}{a} (m\hat{\mathbf{x}} + n\hat{\mathbf{y}}), \qquad (5)$$

where a is the lattice constant of the surface unit cell and m and n are integers.

The quantities ΔE and $\mathbf{K}$ characterize an inelastic scattering event. In a ΔE vs K plot, the locus of points which satisfy the conservation of energy and momentum relations for a single-phonon interaction [i.e., one in which the summations in Eqs. (3) and (4) contain only a single term] defines the "scan curve" which for the present "in-plane" experimental geometry (in which the incident beam, the scattered beam, and the normal to the surface lie in the same plane) is given by

$$\frac{\Delta E}{E_i} = \frac{1}{\sin^2 \theta_f} [\sin \theta_i + (K/K_i)]^2 - 1. \qquad (6)$$

The intersection points of the scan curve with the extended-zone plot of the phonon dispersion curves represent the kinematically accessible phonons that can be observed as single-phonon peaks in a time-of-flight spectrum. Scattering events which are described by Eqs. (3) and (4) with more than one term in the summations are the subject of the theory described in the next section.

III. THEORY

The quantum-mechanical theory for the analysis of the multiphonon background has been developed previously.[32,33] We briefly review the important features here. The interaction between an atomic projectile and a surface can be described by a Hamiltonian of the form

$$H = H^p + H^c + V, \qquad (7)$$

where H^p is the Hamiltonian of the free particle, H^c is the Hamiltonian of the unperturbed crystal, and V is the interaction coupling the projectile and crystal.

In these experiments, the experimentally measured quantity is the three-dimensional differential reflection coefficient $d^3R/d\Omega_f dE_f$, which gives the fraction of the incident particles that are scattered into a small final solid angle $d\Omega_f$ and over a final energy interval E_f to $E_f + dE_f$. The standard approach is to start with the quantum-mechanical probability density for the projectile to lose or gain an amount of energy ΔE, or to start from the generalized golden rule for the transition rate for scattering from projectile state $\mathbf{k}_i$ to state

$\mathbf{k}_f$.[17,34–37] In general, starting from the Hamiltonian of Eq. (7) either approach leads to a differential reflection coeffi-

cient which can be expressed in terms of a generalized displacement correlation function $\mathscr{W}$,[17,33]

$$\frac{d^3R}{d\Omega_f dE_f} = \frac{k_f k_{fz}}{(2\pi)^3 \hbar L^2} \sum_{\mathbf{G}} \int_{-\infty}^{+\infty} dt \int d\mathbf{R} \int d\mathbf{R}' e^{i[(\mathbf{K}+\mathbf{G})\cdot(\mathbf{R}-\mathbf{R}')-\Delta Et/\hbar]} |\sigma_{fi}|^2 \sum_l e^{i\mathbf{K}\cdot\mathbf{R}_l} e^{-W(\mathbf{R},\mathbf{k})} e^{-W(\mathbf{R}',\mathbf{k})} e^{2\mathscr{W}_l(\mathbf{R},\mathbf{R}',t)}, \quad (8)$$

where we have denoted the scattering vector in the usual way, $\mathbf{k} = \mathbf{k}_f - \mathbf{k}_i$, and where $\exp[-W(\mathbf{R},\mathbf{k})]$ is the Debye-Waller factor whose argument is the self-correlation function of a point on the surface evaluated at equal times, $W(\mathbf{R},\mathbf{k}) = \mathscr{W}_0(\mathbf{R},\mathbf{R},t=0)$.

For carrying out tractable calculations, further approximations must be made. A combination of the trajectory approximation, with trajectories limited to classical paths, and the quick-collision approximation leads to an expression in which the correlation function of Eq. (8) becomes the ordinary displacement correlation function:[33]

$$\frac{d^3R}{d\Omega_f dE_f} = \frac{k_f k_{fz}}{(2\pi)^3 \hbar L^2} \sum_{\mathbf{G}} \int_{-\infty}^{+\infty} dt \int_{\text{u.c.}} d\mathbf{R} \int_{\text{u.c.}} d\mathbf{R}' e^{i[(\mathbf{K}+\mathbf{G})\cdot(\mathbf{R}-\mathbf{R}')-\Delta Et/\hbar]}$$

$$\times |\sigma_{fi}|^2 \sum_l e^{i\mathbf{K}\cdot\mathbf{R}_l} e^{-W(\mathbf{R},\mathbf{k})} e^{-W(\mathbf{R}',\mathbf{k})} e^{\langle\langle \mathbf{k}\cdot\mathbf{u}_0(\mathbf{R},0)\mathbf{k}\cdot\mathbf{u}_l(\mathbf{R}',t)\rangle\rangle} \quad (9)$$

with the Debye-Waller exponent taking on the classic form

$$2W(\mathbf{R},\mathbf{K}) = \langle\langle[\mathbf{k}\cdot\mathbf{u}_l(\mathbf{R},t)]^2\rangle\rangle, \quad (10)$$

where u.c. denotes a surface unit cell. Within these approximations the scattering amplitude σ_{fi} of Eq. (9) is identified as the transition matrix for a unit cell of the elastic part of the perturbing potential V, extended off the energy shell. The most severe of the approximations leading to Eq. (9) would appear to be the quick-collision approximation which assumes that the time spent by the projectile near the surface is short compared to a phonon period. This condition is not obeyed for high-energy phonons, and thus such an approximation is not well justified for calculating single-phonon exchanges. However, the multiphonon intensity is dominated by exchange of low-energy phonons, and thus for this contribution the quick-collision approximation becomes reasonable.[38]

The exponential of the displacement correlation function in Eq. (9) can be expanded to yield different phonon contributions. The elastic and single-phonon contributions are obtained upon extending the exponential in a Taylor series in its argument to zero and first order in the displacement correlation function, respectively. The multiphonon part consists of the remaining terms in the expansion.

A. Model calculations

In the semiclassical limit, the assumption that long-wavelength phonons contribute most strongly to the multiphonon intensity[32,33] leads to a further simplification. This consists of expanding the lattice displacement in a series of $\mathbf{Q}\cdot\mathbf{R}_l$, where $\mathbf{R}_l$ is the component of $\mathbf{r}_l$ parallel to the surface. Then the differential reflection coefficient can be cast into the following form, using the notation $\Delta E = \hbar\omega$:[32]

$$\frac{d^3R}{d\Omega_f dE_f} = \frac{m^2|\mathbf{k}_f|}{8\pi^3\hbar^5 k_{iz}} |\tau_{fi}|^2 e^{-2W(\mathbf{k})} S(\mathbf{K},\omega) I(\mathbf{K},\omega), \quad (11)$$

namely, the product of a form factor $|\tau_{fi}|^2$, a Debye-Waller factor, a structure factor $S(\mathbf{K},\omega)$ due to periodicity of the surface, and an energy exchange factor $I(\mathbf{K},\omega)$. For the purposes of the present work it is sufficient to evaluate the structure factor and the energy exchange factor in terms of a Debye phonon distribution, resulting in

$$S(\mathbf{K},\omega) = \sum_l e^{-i\mathbf{K}\cdot\mathbf{R}_l} \exp\left[\frac{-\omega_0 k_B T \mathbf{R}_l^2}{2\hbar v_R^2}\right], \quad (12)$$

and

$$I(\mathbf{K},\omega) = \int_{-\infty}^{+\infty} dt\, e^{-i(\omega+\omega_0)t} \exp\left[\frac{2W(\mathbf{k})\sin(\omega_D t)}{\omega_D t}\right], \quad (13)$$

where v_R is a weighted average of phonon velocities parallel to the surface and is approximately the Rayleigh velocity for the surface modes near the zone center, ω_D is the Debye frequency, and T is the surface temperature. The semiclassical energy shift is given by $\hbar\omega_0 = \hbar^2 k^2/2M$ where M is the crystal atom mass. In deriving Eqs. (11), (12), and (13) the high-temperature limit has been employed for the calculations to compare with the data. The high-temperature approximation to the semiclassical limit is applicable when the temperature is above one-half the Debye temperature of the crystal.[39]

For the form factor $|\tau_{fi}|^2$, we have adopted expressions obtained from the distorted-wave Born approximation for single-phonon scattering, namely, a Mott-Jackson matrix element for perpendicular motion and a cutoff factor for parallel motion:[40–42]

$$|\tau_{fi}|^2 = e^{-K^2/Q_c^2} v_{\text{MJ}}^2(k_{fz}, k_{iz}). \quad (14)$$
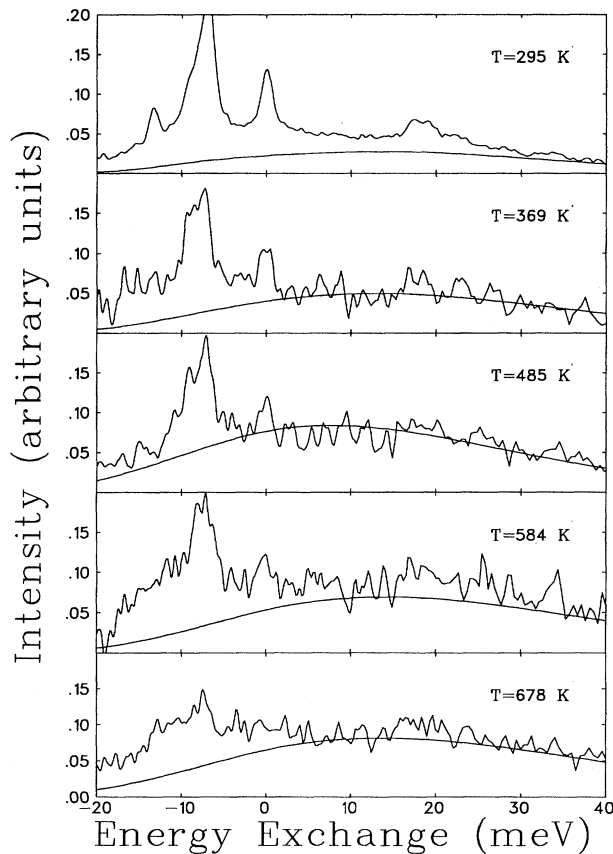
FIG. 1. Plots of scattered intensity vs energy exchange for the He/LiF(001)⟨100⟩ system at 40° incidence angle and for a range of crystal temperatures. The smooth lines are the theoretical fits to the data which are shown by the jagged lines. The relevant parameters are $E_i = 32$ meV, Debye temperature $= 520$ K, crystal mass $= 12.97$ amu, $\beta = 6.0$ Å^{-1}, and $Q_c = 4.5$ Å^{-1}. The large peak in the intensity near -8 meV is due to inelastic single-phonon scattering while the smaller one at zero energy exchange for the lower-temperature spectra arises from a diffuse elastic contribution. The calculated curve excludes the elastic and single-phonon scattering terms.

The Mott-Jackson factor v_{MJ} is the matrix element of the one-dimensional potential $v(z) = \exp(-\beta z)$ taken with respect to its own distorted eigenstates.

IV. RESULTS

Unless the temperature is very low, the multiphonon background appears as a smooth, broad foot underneath the elastic and single-phonon peaks in energy-resolved spectra, and exhibits a well-defined maximum peak intensity and width (measured as the full width at half maximum, FWHM).

Figure 1 is a comparison of the experimental data with the calculations using the semiclassical relations for a range of temperatures at a 40° angle of incidence (nonspecular scattering). At high temperatures the multiphonon background dominates the scattering. The diffuse elastic peak, which is almost invisible at high temperatures, steadily increases as the temperature decreases. A similar effect can be seen for the single-phonon inelastic peak that appears at $\Delta E = -8$

meV. At the higher temperatures the theoretical calculations appear to predict the multiphonon background rather well. At the lowest temperature studied (295 K), the shape of the theoretical curve still follows the experimental data though it lies somewhat below the measured curve. The difference between the theoretical calculations and the experimental results at low temperatures can, at least partially, be attributed to significant contributions in the scattering from single-phonon interactions, particularly the bulk-projected single-phonon modes which have been excluded from the calculations.

All of the calculations reported in this paper are based on a Debye frequency distribution function for the phonon correlation functions with the value 520 K used for the surface Debye temperature. The value 520 K was chosen as approximately the bulk Debye temperature of $\Theta_D = 734$ K (Ref. 27) divided by the square root of 2, which is a standard way of estimating the surface Debye temperature.[29] The two parameters in the form factor are the range parameter of the exponential repulsive potential β and the cutoff parameter of the potential Q_c. A fit to the data resulted in values of $\beta = 6.0$ Å^{-1} and $Q_c = 4.5$ Å^{-1}. Both of these parameters are somewhat larger than those determined from the relative intensities of the diffraction peaks and are at the upper end of the range obtained from single- and multiple-phonon scattering from metal surfaces.[38] However, they are consistent with values obtained previously for multiphonon scattering from alkali halide insulators. For example, a previous (and more restrictive) He-scattering study of the NaCl surface produced $\beta = 5.6$ Å^{-1} and Q_c greater than 10 Å^{-1}.[42] Large values of β imply a rather stiff repulsive potential and large values of Q_c imply a strongly corrugated surface which can scatter particles with large parallel momentum exchanges (which usually correspond to large angular deviations from the specular direction). It is important to note that these parameters, within the approximations employed in the treatment here, determine the intensities and shapes of the multiphonon scattering intensities for all incident angles and for all surface temperatures. No other adjustments or scalings are made.

Figure 2 shows the data and theoretical comparison for the specular angle of incidence (45°). Some discrepancy is present at low temperatures, which could be due to the difficulty in accurately measuring the small inelastic background underneath the very large elastic peak that occurs at specular incidence. Figure 3 which is for 50° incidence angle exhibits similar results to those shown in Fig. 1; namely, the agreement improves with decreasing contribution of the single-phonon scattering as the temperature is raised.

The results shown in Figs. 1–3 are a small subset of the large number of incident angles and surface temperatures which were measured. They have been selected since they illustrate the results of the scattering at subspecular, specular, and supraspecular angles of incidence, respectively. To make quantitative assessments of the comparisons made for the entire measured range of temperatures and angles, we have summarized the results in Figs. 4 and 5 in terms of maximum multiphonon peak intensities and the FWHM's.

The maximum intensity of the multiphonon background is compared in Fig. 4 for the whole range of temperatures and for a selection of incidence angles over the range of incident
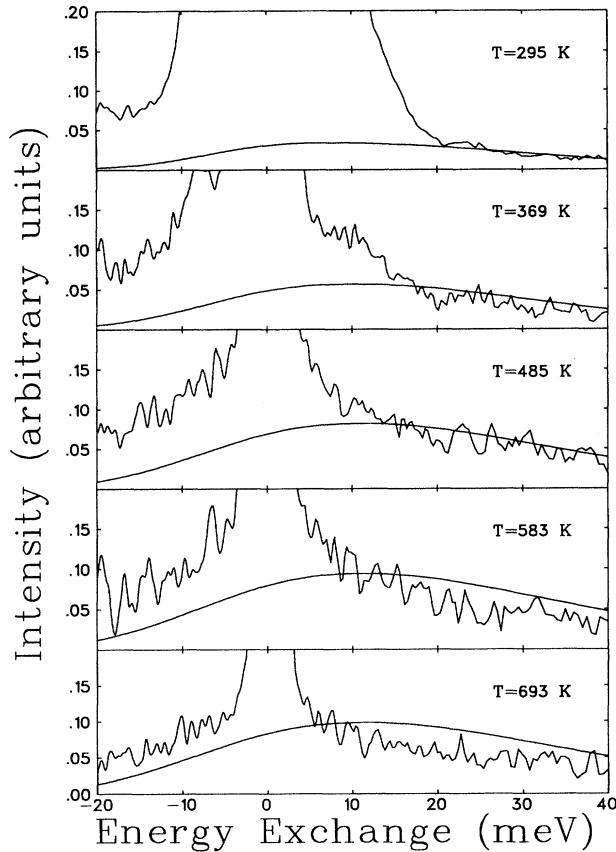
FIG. 2. Plots of scattered intensity vs energy exchange for the He/LiF(001)⟨100⟩ system at 45° (specular) incidence. All other parameters are the same as in Fig. 1. The large intensity at zero energy exchange comes mostly from the specular elastic contribution with a very much smaller diffuse elastic component.

FIG. 3. Plots of scattered intensity vs energy exchange for the He/LiF(001)⟨100⟩ system at 50° incidence. All other parameters are the same as in Fig. 1. The peak near +10 meV is from a single-phonon inelastic scattering process while the peak at zero energy exchange is from diffuse elastic scattering. The calculated curve does not include these two contributions.

angles studied. The peak height of the experimental multiphonon foot was estimated from the data. With the exception of the specular angle at 45°, discrepancies between experiment and theory are present only at low temperatures. This is probably due, in large part, to the difficulty in measuring the multiphonon background near prominent elastic and single-phonon peaks, and to the contribution from bulk single-phonon scattering. The discrepancy at high temperature at the specular angle is very likely due to the difficulty in distinguishing the experimental multiphonon intensity from the residual tail of the beam energy spread in the specular elastic intensity.

The peak intensity is an increasing function of T except for measurements near to normal incidence, $\theta_i = 35°$. This implies that the experiment is still well within the quantum regime in which the multiphonon inelastic intensity is growing with T at the expense of the diffraction and single-phonon quantum peaks. At larger temperatures (and higher incident energies) the quantum peaks disappear. This is the beginning of the classical regime which is the point at which the peak of the multiphonon intensity starts to decrease. This decrease is an effect of unitarity, because when all particles are scattered into the classical multiphonon spectrum the maximum intensity will decrease in order to conserve the
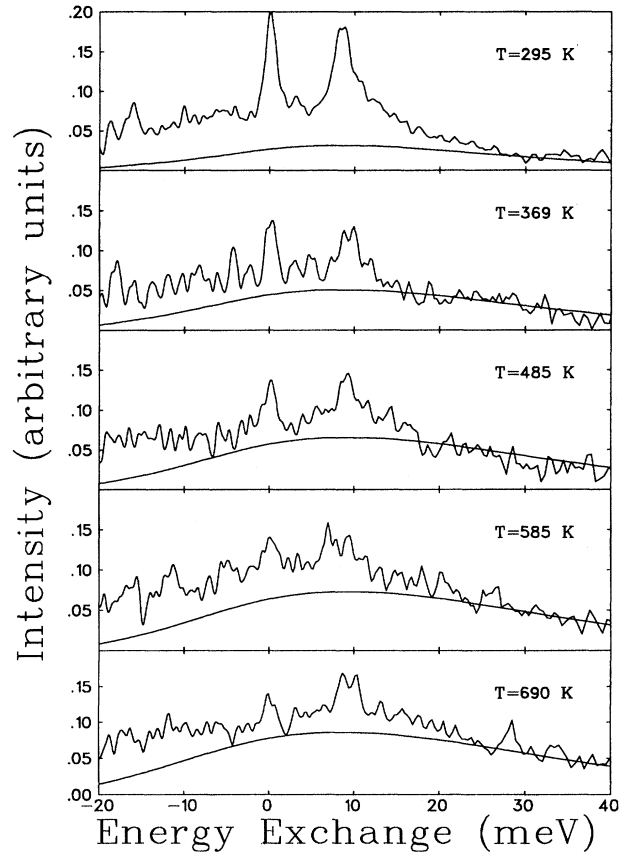
total number of particles as the spectrum spreads over a larger energy transfer range. This expected decrease appears to be occurring at high T for $\theta_i = 35°$, which is the angle of incidence for which the particles strike the surface with the largest normal momentum.

In Fig. 5 the FWHM's for the theory and the estimated experimental multiphonon background are compared for the range of temperatures and for each angle of incidence studied. As expected, the FWHM is a monotonically increasing function of T for all incident angles. Good agreement with theory is observed throughout the range.

V. DISCUSSIONS AND CONCLUSIONS

In this paper we have presented extensive experimental results for the scattering of He from the ⟨100⟩ azimuth of a LiF(001) surface in an energy and temperature range in which the diffuse inelastic background is important. The experimental results for the diffuse inelastic background have been analyzed with a multiphonon scattering theory. Good agreement is obtained with the semiclassical version of the theory over a large range of incident angles of the He beam and over a range of temperatures extending from well below
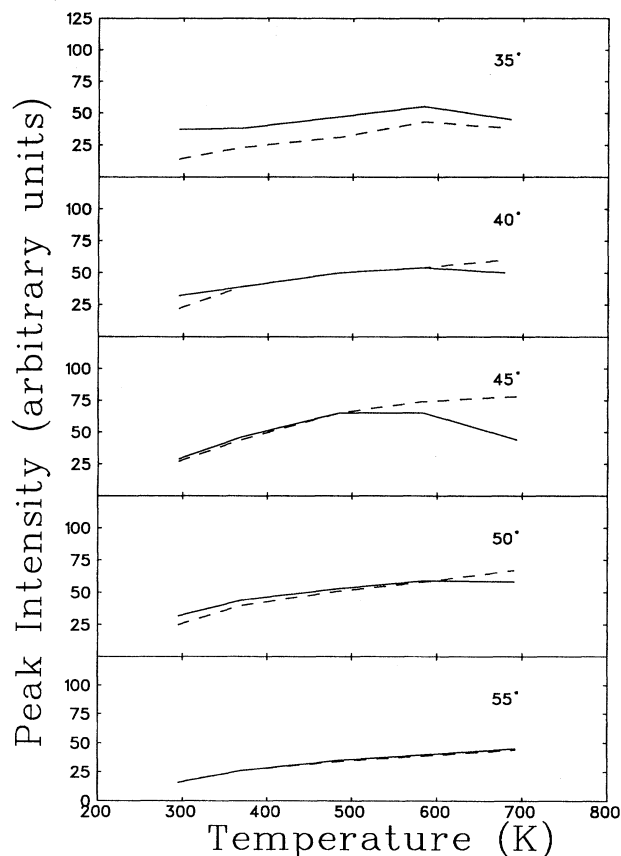
FIG. 4. Comparison of the relative multiphonon peak intensity vs temperature for different angles of incidence for the He/LiF(001) $\langle 100 \rangle$ scattering system. The dashed lines are the theoretical fits to the data which are represented by solid lines.

FIG. 5. FWHM vs temperature for different angles of incidence for the He/LiF(001)$\langle 100 \rangle$ scattering system. The dashed lines are the theoretical fits to the data which are represented by solid lines.

to near the bulk Debye temperature of LiF. The theory does an even better job of predicting the temperature and angular dependence of the global features of the diffuse inelastic distribution, namely, its maximum intensity and full width at half maximum.

For the actual calculations carried out in this study the phonon spectral density of LiF was represented by a Debye frequency distribution. The satisfactory results obtained by using such a simple model for the phonons indicate two important aspects of the diffuse inelastic background. First, for such clean and ordered surfaces as the cleaved LiF studied here, the diffuse inelastic background at temperatures above half the bulk Debye temperature is largely due to the multiphonon contributions. Secondly, the multiphonon contribution to the diffuse inelastic background for such surfaces appears nearly independent of the details of the phonon spectral density. This latter point is important to the analysis of He scattering data because it suggests that in many cases the inelastic background can be predicted using simple phonon models such as the Debye frequency distribution. If multiphonon calculations required using more realistic phonon spectral densities, they would involve very lengthy numerical calculations and extensive amounts of computer time, which would be distinctly disadvantageous.

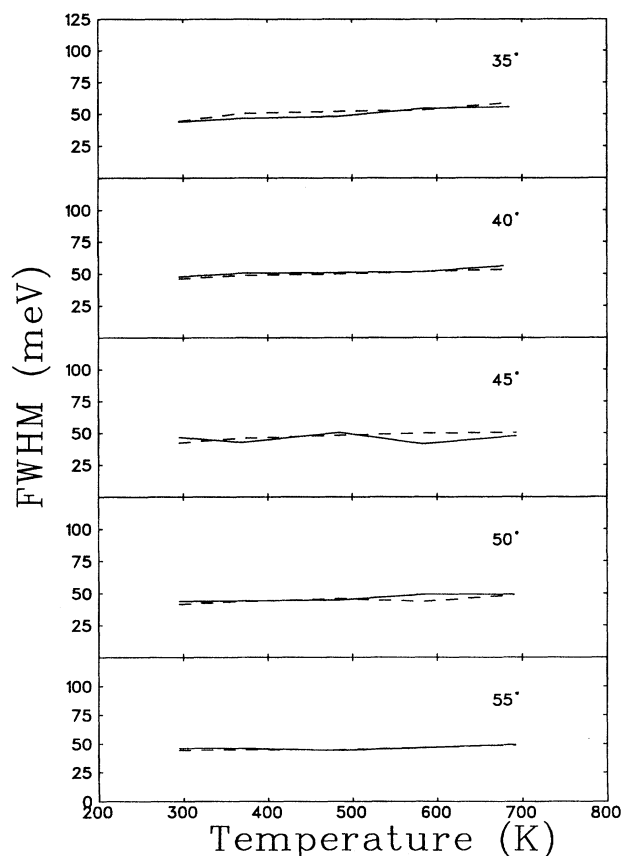The comparison of theory with experiment also gives im-

portant information about the interaction potential between the He projectiles and the surface through determination of the form factor for inelastic scattering. Here, as a theoretical model, we have adopted the form factor which has been widely used for single- as well as multiphonon scattering from metal surfaces, namely, the product of a cutoff function and the Mott-Jackson matrix element for an exponentially repulsive potential. The values of the parameters determined by fitting the data to the theory over a large range of incident polar angles θ_i are $\beta = 6.0$ Å^{-1} for the stiffness parameter of the potential and $Q_c = 4.5$ Å^{-1} for the cutoff parameter. The value of β comes at the upper end of the range determined in single- and multiphonon scattering studies of metal surfaces,[38] and is consistent with previous measurements of multiphonon scattering from alkali halide insulators.[42] This large value of β implies a stiffer potential than that which is normally determined from purely elastic diffraction studies of similar surfaces. Our value of Q_c is substantially larger than the 1–2 Å^{-1} range usually found for metals,[38] but is consistent with previous studies of other alkali halides.[42] A large value of Q_c implies a negligible cutoff with parallel momentum exchange and this is consistent with a highly corrugated surface which is capable of scattering incoming particles out to large angular deviations away from the specular direction. In the previous measurements and comparisons to theory,[42] the Q_c value was found to be large and

somewhat insensitive to the fit. However, in this work which covered a wide range of incident angles, the range of this parameter was considerably narrowed. Thus in determining the parameters of the form factor, β and Q_c, it is important to carry out the multiphonon experiments at angles other than the specular incidence.

These two properties of the multiphonon inelastic background, that it is relatively independent of the details of the phonon distribution and that it gives the form factor for inelastic scattering, have important implications for more detailed studies of the single-phonon scattering intensities. In principle, a study of the intensities of single-phonon transitions is a method for measuring the surface phonon spectral density. However, the theoretical interpretation of such experiments is complicated by the fact that the intensity depends directly on both the phonon spectral density and on the form factor. The form factor for atom-surface scattering is not simple, and, like the phonon spectral density, is also a rapidly varying function of energy and momentum. Thus

without prior knowledge of the form factor it is not possible to unambiguously extract the phonon spectral density from the data. As is evident from the present work, the multiphonon intensity does give an unambiguous determination of the form factor (in the semiclassical regime) because the multiphonon intensity is essentially independent of the phonon spectral density. Furthermore, in the context of the semiclassical theory presented here this form factor is the same as that for the single-phonon part of the scattering intensity. Thus the multiphonon intensity provides a first-order approximation to the form factor needed, in combination with more detailed theoretical analysis, to extract the phonon spectral density through comparisons with measured single-phonon scattered intensities.

ACKNOWLEDGMENTS

[1] O. Stern, Naturwissenschaften 17, 391 (1929).

[2] I. Estermann and O. Stern, Z. Phys. 61, 95 (1930).

[3] I. Estermann, R. Frisch, and O. Stern, Z. Phys. 73, 348 (1931).

[4] J. M. Jackson and N. F. Mott, Proc. R. Soc. (London) Ser. A 137, 703 (1932).

[5] J. E. Lennard-Jones and A. F. Devonshire, Nature 137, 1069 (1936).

[6] A. F. Devonshire, Proc. R. Soc. (London) Ser. A 156, 37 (1936).

[7] J. N. Smith, Jr., D. R. O'Keefe, H. Saltzburg, and R. L. Palmer, J. Chem. Phys. 50, 4667 (1969).

[8] S. S. Fisher, M. N. Bishara, A. R. Kulthau, and J. E. Scott, Jr., in Rare Field Gas Dynamics, edited by L. Trilling and H. Y. Wachman (Academic, New York, 1969), p. 1227.

[9] R. B. Subbarao and D. R. Miller, J. Chem. Phys. 51, 4679 (1969).

[10] B. R. Williams, J. Chem. Phys. 55, 1315 (1971).

[11] J. B. Anderson and J. B. Fenn, Phys. Fluids 8, 780 (1965).

[12] J. G. Skofronick and W. M. Pope, Rev. Sci. Instrum. 44, 76 (1973).

[13] J. P. Töennies and K. Winkelmann, J. Chem. Phys. 66, 3965 (1977).

[14] D. Eichenauer and J. P. Töennies, J. Chem. Phys. 85, 532 (1986).

[15] H. Hoinkes, Rev. Mod. Phys. 52, 933 (1980).

[16] G. Boato and P. Cantini, Adv. Electron. Electron Phys. 60, 95 (1983).

[17] V. Bortolani and A. C. Levi, Riv. Nuovo Cimento 9, 1 (1986).

[18] J. A. Barker and D. J. Auerbach, Surf. Sci. Rep. 4, 1 (1984).

[19] T. Engel and K. H. Rieder, in Structural Studies of Surfaces, edited by G. Höhler, Springer Tracts in Modern Physics Vol. 91 (Springer-Verlag, Berlin, 1982), p. 55.

[20] R. B. Gerber, Chem. Rev. 87, 29 (1987).

[21] V. Celli, in Many Body Phenomena at Surfaces, edited by D. Langreth and H. Suhl (Academic, New York, 1984), p. 315.

[22] J. P. Töennies, Phys. Scr. T19, 39 (1987).

[23] J. P. Töennies, in Surface Phonons, edited by W. Kress (Springer-Verlag, Heidelberg, 1992), Chap. 5.

[24] R. B. Doak, in Atomic and Molecular Beam Methods, edited by G. Scoles (Oxford University Press, New York, 1992), Vol. 2, Chap. 14.

[25] J. R. Manson and V. Celli, Phys. Rev. B 39, 3605 (1989).

[26] V. Celli, D. Himes, P. Tran, J. P. Toennies, Ch. Wöll, and G. Zhang, Phys. Rev. Lett. 66, 3160 (1991).

[27] J. T. Lewis et al., Phys. Rev. 161, 877 (1967).

[28] G. Chern, J. G. Skofronick, W. P. Brug, and S. A. Safron, Phys. Rev. B 39, 12 828 (1989).

[29] G. Brusdeylins, R. B. Doak, and J. P. Töennies, Phys. Rev. B 27, 3662 (1983).

[30] G. Bracco, M. d'Avanzo, C. Salbo, T. Tatarek, S. Terreni, and F. Tommasini, Surf. Sci. 189/190, 684 (1990).

[31] G. Boato, P. Cantini, and L. Mattera, Surf. Sci. 55, 141 (1976).

[32] J. R. Manson, Phys. Rev. B 43, 6924 (1991).

[33] J. R. Manson, Comput. Phys. Commun. 80, 145 (1994).

[34] J. Böheim and W. Brenig, Z. Phys. B 41, 243 (1983).

[35] K. Burke, B. Gumhalter, and D. Langreth, Phys. Rev. B 47, 12 852 (1993).

[36] R. Brako and D. M. Newns, Phys. Rev. Lett. 48, 1859 (1982).

[37] R. Brako and D. M. Newns, Surf. Sci. 123, 439 (1982).

[38] F. Hofmann, J. P. Toennies, and J. R. Manson, J. Chem. Phys. 101, 10 155 (1994).

[39] Srilal M. Weera and J. R. Manson, J. Electron Spectrosc. Relat. Phenom. 64/65, 707 (1993).

[40] V. Celli, G. Benedek, U. Harten, J. P. Toennies, R. B. Doak, and V. Bortolani, Surf. Sci. 143, L376 (1984).

[41] F. O. Goodman and H. Y. Wachman, Dynamics of Gas-Surface Scattering (Academic, New York, 1976).

[42] G. G. Bishop, W. P. Brug, G. Chern, J. Duan, S. A. Safron, J. G. Skofronick, and J. R. Manson, Phys. Rev. B 47, 3966 (1994).